FATA2025
FAst Timing Applications for Nuclear Physics and Medical Imaging
Catania - Italy, 8th - 10th October 2025

Time of Flight technique for online monitoring of laser-matter interaction in Inertial Confinement experiments

N. Macaluso, G. Petringa, F. Abubaker, L. Guardo, M. La Cognata, E. Pagano, G. Rapisarda, D. Santonocito, S. Agarwal, M. Alonzo, C. Altana, S. Arjmand, D. Bortot, G. Cantone, R. Catalano, M. Cervenak, C. Ciampi, M. Cipriani, G. A. P. Cirrone, F. Consoli, P. Devi, E. Domenicone, R. Dudzak, D. Ettel, P. Gajdos, B. Grau, L. Giuffrida, J. Krasa, M. Krupka, M. Krus, L. Juha, L. Malferrari, D. Margarone, G. Messina, S. Mirabella, G. Morello, A. D. Pappalardo, A. Picciotto, A.M. Raso, R. Rinaldi, M. Rosinski, M. Scisciò, A. Scandurra, S. Singh, P. Tchórz, A. Trifirò and C. Verona

Introduction:

Fusion as Future Energy Source

- **Nuclear Fusion** is a promising path toward a **high-density, low-carbon energy source.**
- Based on light nuclei reactions (e.g. D-T, or p-B11)
- Offers several advantages over fission:
  - **Intrinsically safe**: reactions stop when confinement condition are lost
  - Greatly **reduced long-lived radioactive waste** (virtually none for pB11 reaction)
  - **High energy yield** per unit mass of fuel
- Critical points:
  - **Fuel is not truly unlimited** (tritium must be bred)
  - Boron reactions are **less efficient**
  - Neutron-induced activation remains an issue for most current fusion scheme

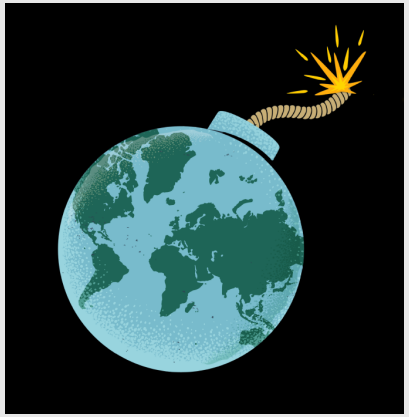

- $D + T \rightarrow \alpha + n + 17.6\ MeV$
- $p + {}^{11}B \rightarrow 3\alpha + 8.6\ MeV$

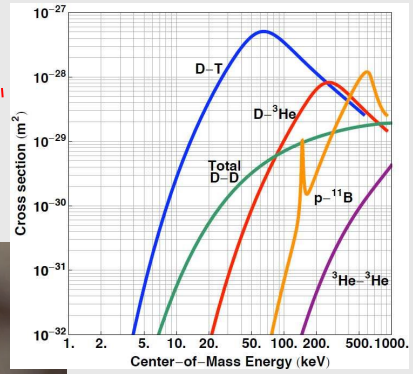

Nicolò Macaluso - nicolo.macaluso@dfa.unict.it
nicolo.macaluso@lns.infn.it

Introduction:

Two main approaches to Fusion

- **Magnetic Confinement Fusion (MCF)**
  - Plasma confined by strong magnetic field, in two main configuration: ***tokamak*** and ***stellarator***
  - Low plasma density: $\sim 10^{19} - 10^{21}\ m^{-3}$
  - Long confinement times (seconds-minutes)
  - Large spatial scales (meters)
- **Inertial Confinement Fusion (ICF)**
  - Plasma confined by rapid implosion using intense laser or particle beams.
  - Extremely high plasma density: $\sim 10^{30} - 10^{33}\ m^{-3}$
  - Extremely short timescale (picoseconds-nanoseconds).
  - Spatial scale (micron to cm)

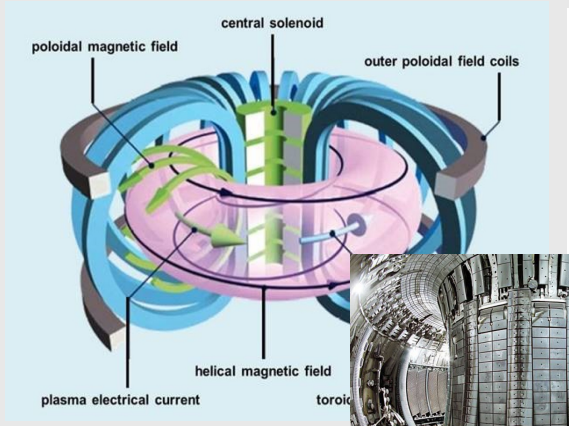

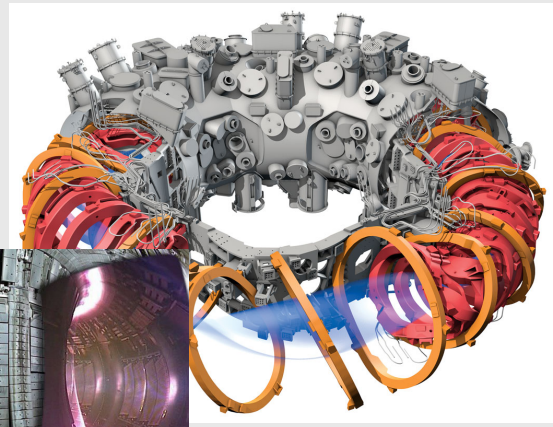

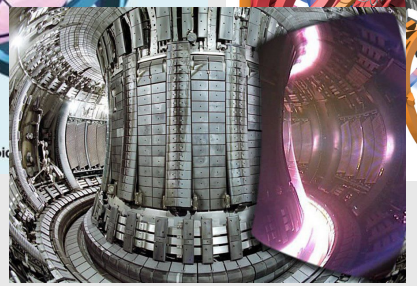

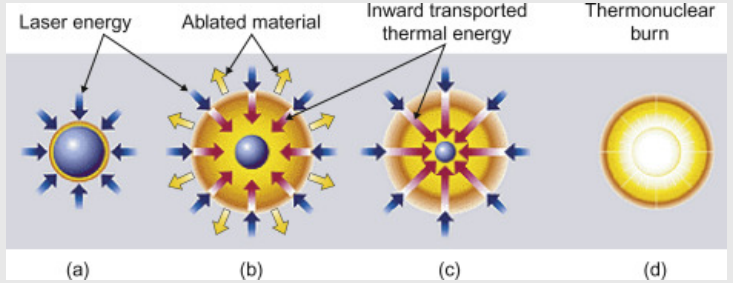

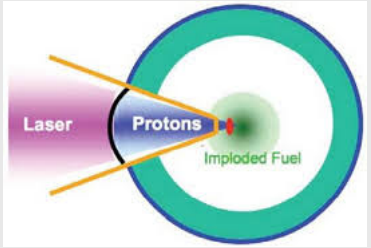

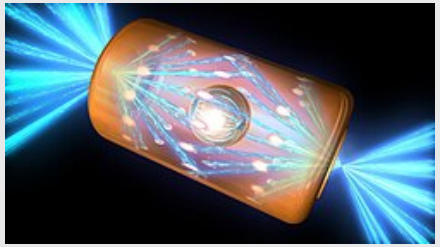

Nicolò Macaluso - nicolo.macaluso@dfa.unict.it
nicolo.macaluso@lns.infn.it

Inertial Confinement Fusion:

- Typically, **Deuterium** and **Tritium** fuel are employed in capsule target.
- D and T are imploded by means of laser or x-ray drive
- This process follows 4 steps:
  1. **Capsule irradiation**
  2. **Ablation**
  3. **Implosion**
  4. **Thermonuclear ignition + Burn**
- Two main technique:
  - **Direct Drive:** lasers directly irradiate the fuel capsule
  - **Indirect Drive:** lasers irradiate an external high-Z case, producing soft X-rays that will drive the compression of the fuel capsule
- In **2022** ignition was first achieved at **NIF laboratory**: **3.15 MJ** fusion generated from **2.05 MJ** laser input.

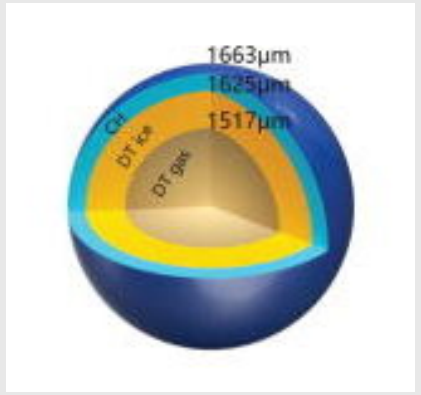

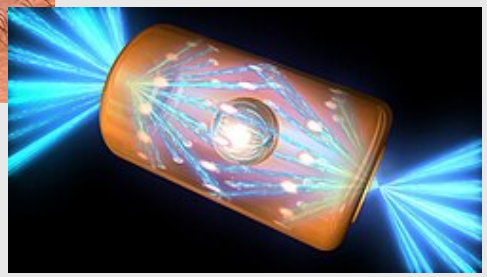

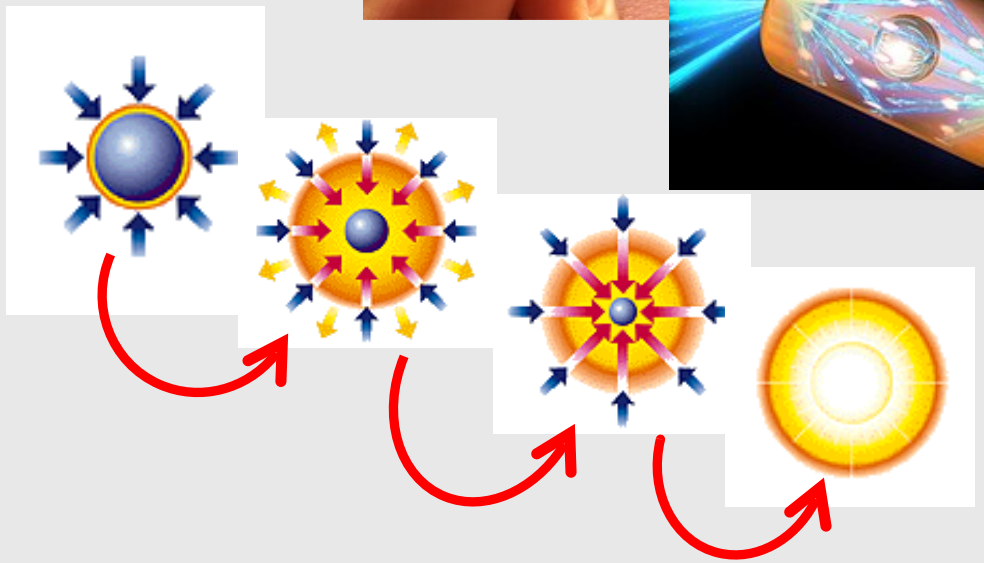

Nicolò Macaluso - nicolo.macaluso@dfa.unict.it
nicolo.macaluso@lns.infn.it

Ion Acceleration Mechanism:

All acceleration mechanism lies on the rapid displacement of target electrons as consequence of the interaction between the high intensity laser radiation and the target.

Divided by the different laser intensity regime in which they occur:

- **Target Normal Sheath Acceleration** (TNSA)
- **Coulomb Explosion** (CE)
- **Radiation Pressure Acceleration** (RPA)

Source characteristics:

- **Compact accelerator** (μm distances)
- **Short duration** (up to fs)
- **Brightness** in terms of fluence ~ $10^{10} - 10^{13}\ str^{-1}$
- **Broad band energy spectrum**
- Not only one ion specie (depends on the target, typically H,C or O)
- Angular aperture up to 40°

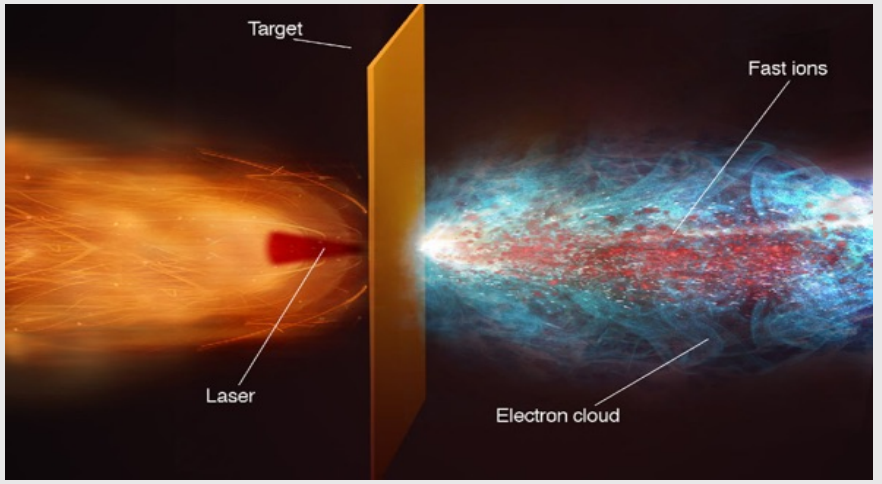

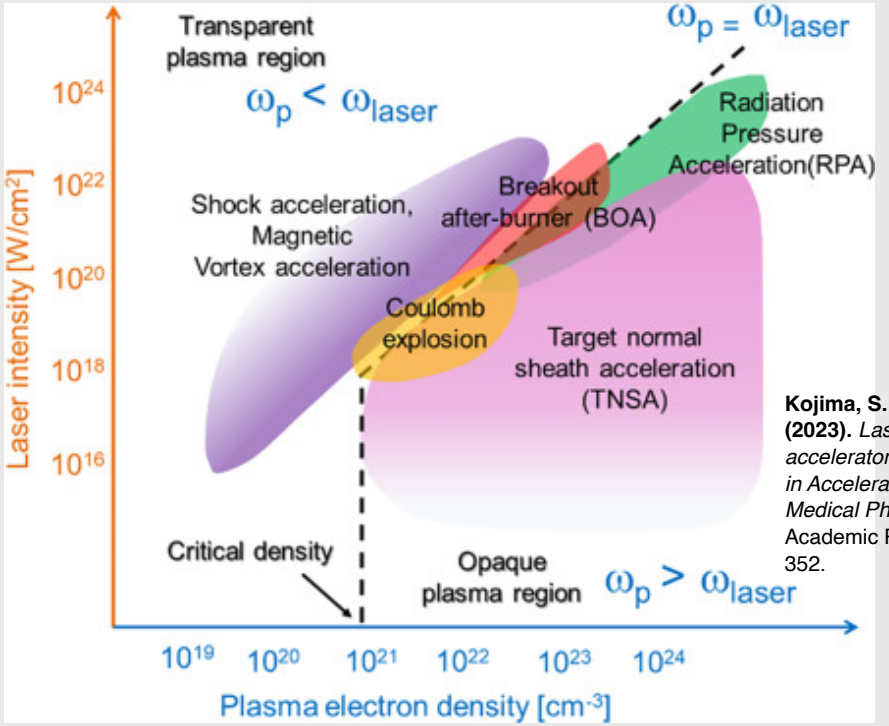

Kojima, S. & Hata, M. (2023). *Laser-driven ion accelerator.* In *Advances in Accelerators and Medical Physics*, Academic Press, pp. 343 352.

Nicolò Macaluso - nicolo.macaluso@dfa.unict.it
nicolo.macaluso@lns.infn.it

TNSA:

- **Micrometer-scale acceleration process** occurring at the rear surface of the target.
- **Dominant mechanism** from moderate ($10^{16} - 10^{18} W/cm^2$) up to high laser intensities ($\sim 10^{21}\ W/cm^2$)
- **Acceleration fields** on the order of $10^{13}\frac{V}{m}\left(\approx \frac{TV}{m}\right)$
- Acts primarily on **surface contaminants** : mainly **Hydrogen, Carbon and Oxygen**
- **Source size**: few tens of micron, << target size
- **Typical divergence**: 10° - 40°
- **Maximum recorded proton energy**: $\sim 100\ MeV$ for laser intensity > $10^{21} W/cm^2$
- **Scaling law**: $E_{p,max} \propto (I_L\ \lambda^2)^{\frac{1}{2}}$

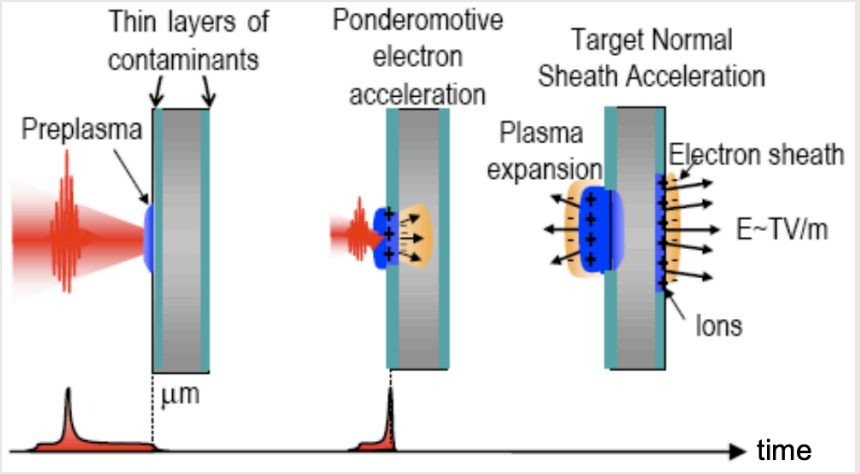

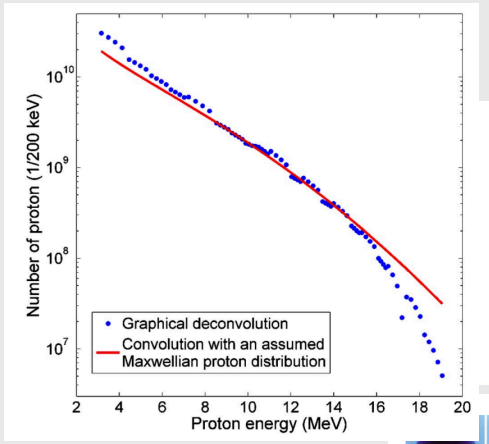

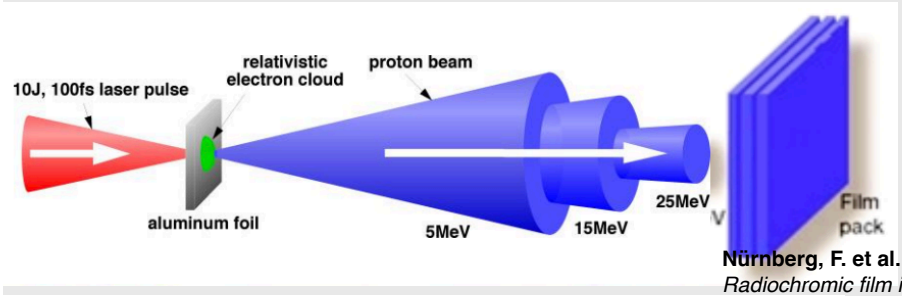

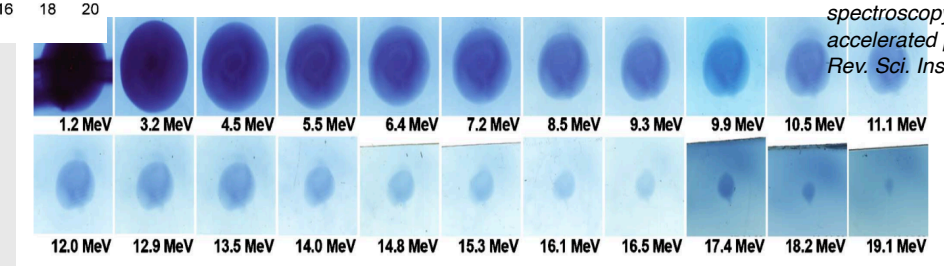

Nürnberg, F. et al. (2009). *Radiochromic film imaging spectroscopy of laser-accelerated proton beams. Rev. Sci. Instrum.*, **80**(3).

$p(^{11}B, 2\alpha)\alpha$ reaction:

- **Reaction**
  - $p + ^{11}B \rightarrow 3\alpha + Q$
  - Energy released: Q = 8.7 MeV
- **Reaction Characteristics**
  - Sharp peak at **165 keV**
  - Broad peak at **660 keV** → *main resonance* $\sigma_{max} \sim 1.4\ b$
- **Reaction Mechanism**
  - The process occurs in two steps:
    1. **Formation of an excited carbon nucleus**:

    2. **Decay of the excited state :**
    proceeds through the sequential breakup producing three alpha particles:

    Or

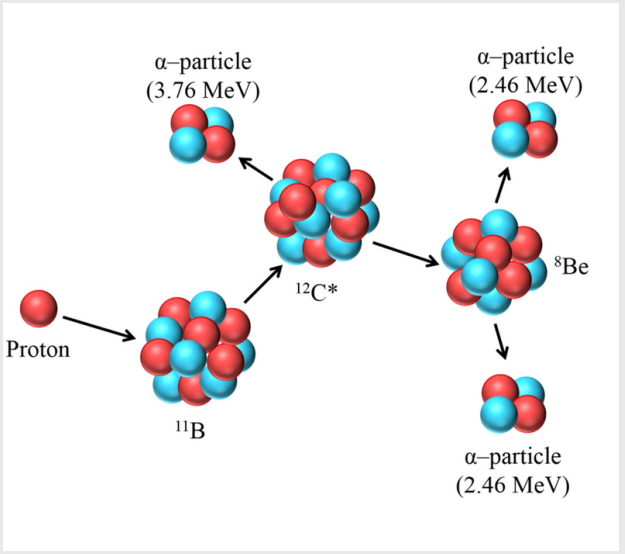

Table 1.1 Some important fusion reactions and parameters of the cross-section factorization 1.21.

	Q (MeV)	$\langle Q_\nu \rangle$ (MeV)	$S(0)$ (keV barn)	$\epsilon_G^{1/2}$ (keV$^{1/2}$)
Main controlled fusion fuels				
$D + T \rightarrow \alpha + n$	17.59		1.2×10^4	34.38
$D + D \rightarrow$ T + p	4.04		56	31.40
$D + D \rightarrow$ ^{3}He + n	3.27		54	31.40
$D + D \rightarrow \alpha + \gamma$	23.85		4.2×10^{-3}	31.40
$T + T \rightarrow \alpha + 2n$	11.33		138	38.45
Advanced fusion fuels				
$D + {}^3He \rightarrow \alpha + p$	18.35		5.9×10^3	68.75
$p + {}^6Li \rightarrow \alpha + {}^3He$	4.02		5.5×10^3	87.20
$p + {}^7Li \rightarrow 2\alpha$	17.35		80	88.11
$p + {}^{11}B \rightarrow 3\alpha$	8.68		2×10^5	150.3
The p–p cycle				
$p + p \rightarrow D + e^+ + \nu$	1.44	0.27	4.0×10^{-22}	22.20
$D + p \rightarrow {}^3He + \gamma$	5.49		2.5×10^{-4}	25.64
$^3He + {}^3He \rightarrow \alpha + 2p$	12.86		5.4×10^3	153.8
CNO cycle				
$p + {}^{12}C \rightarrow {}^{13}N + \gamma$	1.94		1.34	181.0
$[{}^{13}N \rightarrow {}^{13}C + e^+ + \nu + \gamma]$	2.22	0.71	—	—
$p + {}^{13}C \rightarrow {}^{14}N + \gamma$	7.55		7.6	181.5
$p + {}^{14}N \rightarrow {}^{15}O + \gamma$	7.29		3.5	212.3
$[{}^{15}O \rightarrow {}^{15}N + e^+ + \nu + \gamma]$	2.76	1.00	—	—
$p + {}^{15}N \rightarrow {}^{12}C + \alpha$	4.97		6.75×10^4	212.8
Carbon burn				
$^{12}C + {}^{12}C \rightarrow$ ^{23}Na + p	2.24			
$^{12}C + {}^{12}C \rightarrow$ ^{20}Ne + α	4.62		8.83×10^{19}	2769
$^{12}C + {}^{12}C \rightarrow$ ^{24}Mg + γ	13.93			

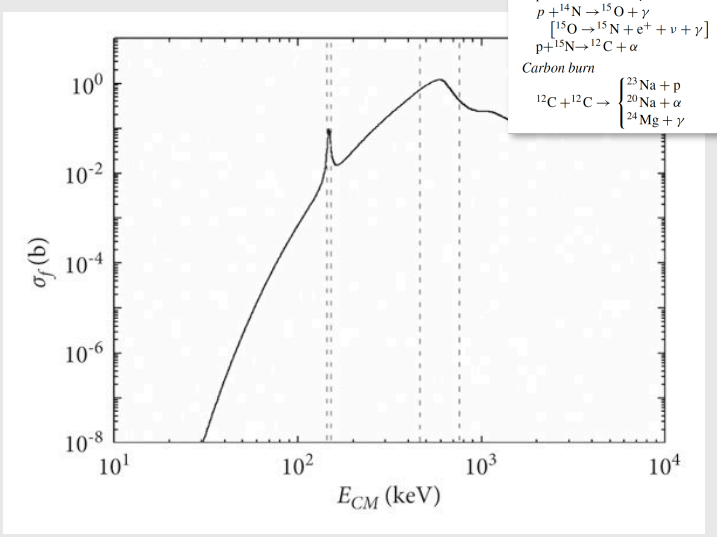

Atzeni, S. & Meyer-Ter-Vehn, J. (2004). *The Physics of Inertial Fusion.* Oxford Science Publications.

Nicolò Macaluso - nicolo.macaluso@dfa.unict.it
nicolo.macaluso@lns.infn.it

$p(^{11}B, 2\alpha)\alpha$ reaction:

- **Energy Spectrum**
  - The summed energy spectrum of the three alpha particles forms a continuum that extends up to $\sim 6.7\ MeV\ (\alpha_0\ peak)$ at the maximum of the cross section
  - It is strongly peaked around $4\ MeV,\ (\alpha_1\ peak)$: on average, two α – particles are emitted at $\sim 4\ MeV$ and one at $\sim 1\ MeV$
- **Angular Distribution**
  - At the $E_p = 675\ keV$ resonance, the emission is isotropic
  - Anisotropies may appear at other protons energies with varying degrees of intensity

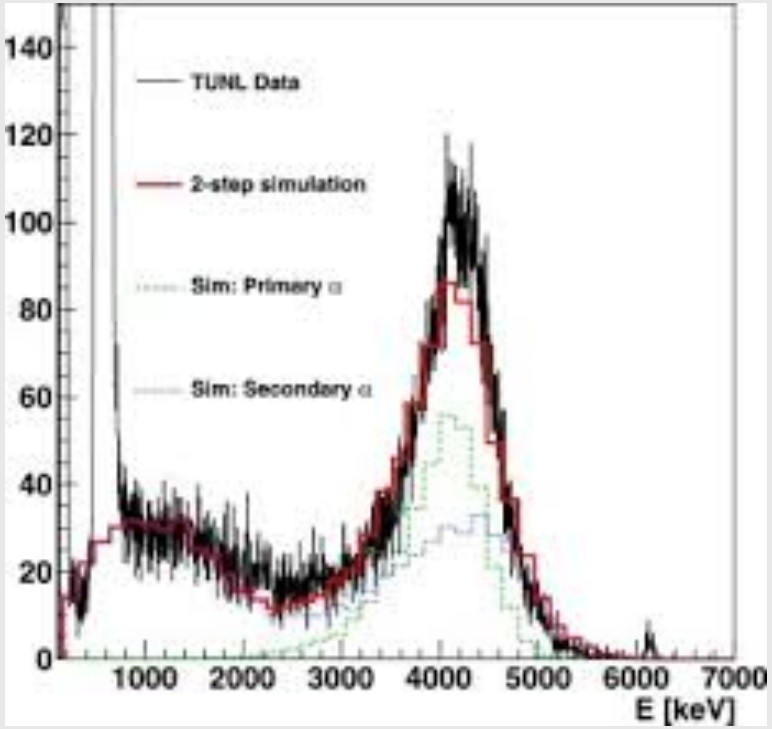

Stave, S. et al. (2011). *Understanding the B¹¹(p, α)αα reaction at the 0.675 MeV resonance. Phys. Lett. B*, **696**(1–2), 26–29.

Laser-Driven experiment: two main scheme adopted

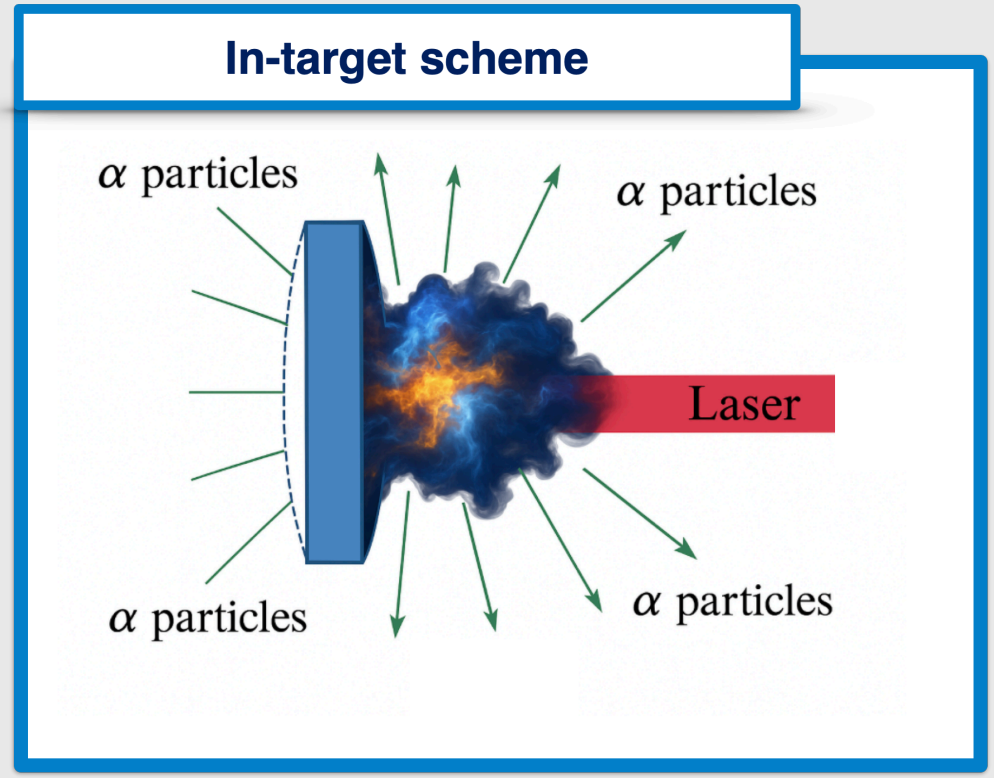

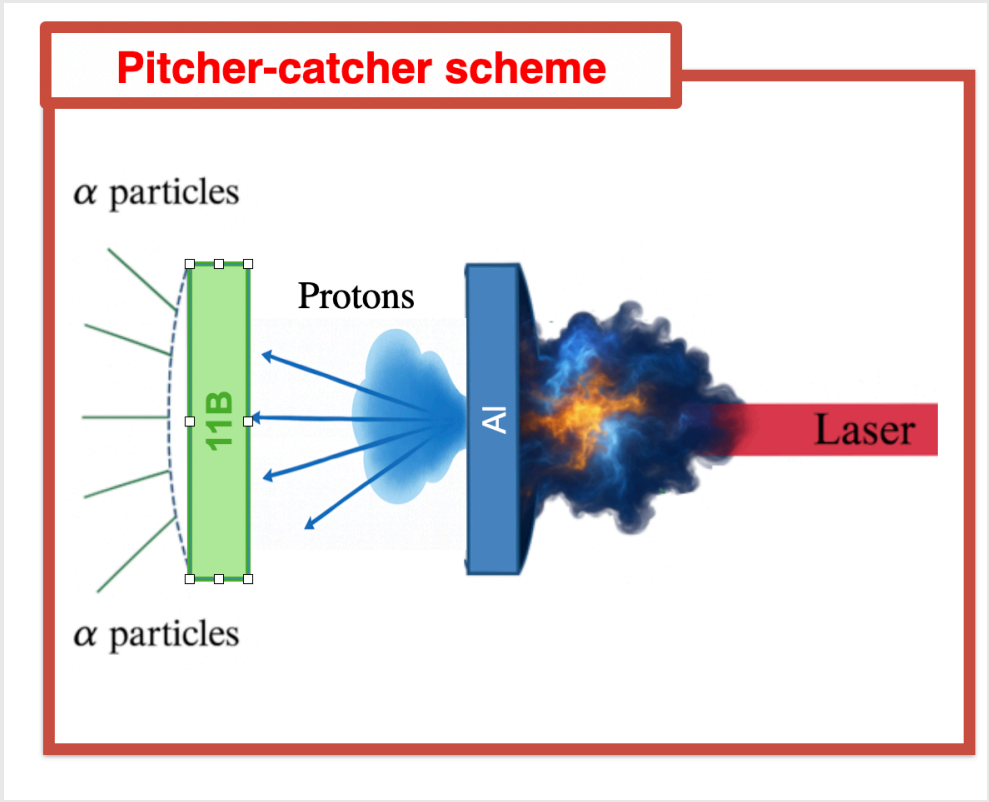

Laser-driven experiments: ion diagnostics

➢ **Thompson Spectrometer**
- **Ion discrimination:** separating ions by their Z/A ration. Enables accurate proton spectrum reconstruction, although ions species with same charge-to-mass ratio overlap their signals
- **EMP sensitivity**

➢ **CR39 nuclear track detector**
- **Passive detector** that records the damage trails left by charged particles in polymer material
- **Particle identification** possible after careful calibration, though unambiguous discrimination is often challenging
- **Offline and time consuming** measurement process (chemical etching and microscopic analysis)
- **Insensitive to EMP noise**, making it suitable for harsh experimental environments

➢ **Time of Flight**

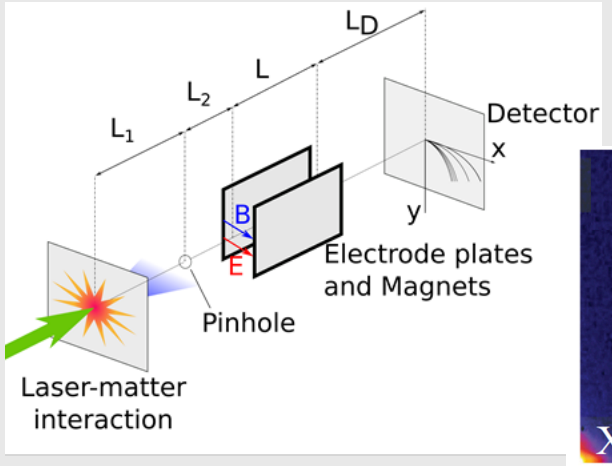

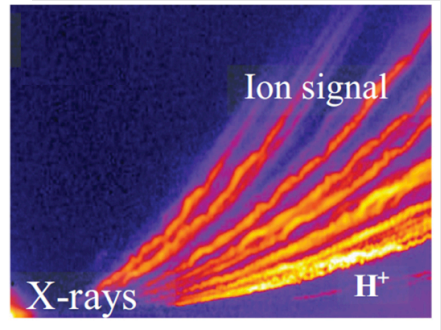

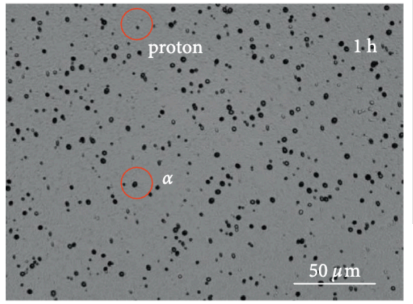

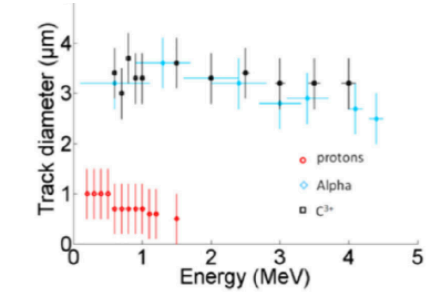

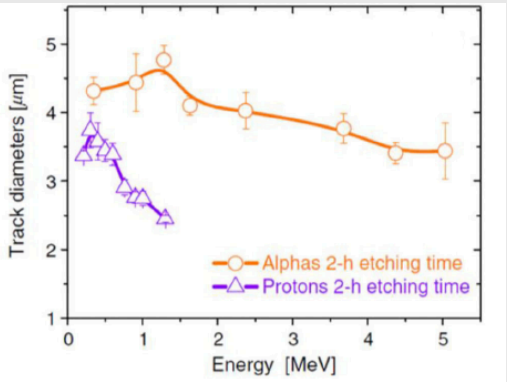

Nicolò Macaluso - nicolo.macaluso@dfa.unict.it
nicolo.macaluso@lns.infn.it

Ion Diagnostics: TOF technique in Laser driven experiments

- Time of Flight detectors are widely used in laser-driven ion acceleration experiments.
- Their **fast response** and **radiation hardness** makes them ideal for **online monitoring** of the laser-matter interaction and for studying ion emission.
- In these experiments, ToF detectors operate in **current mode**, rather than in conventional single-particle mode, due to the **high particle fluence over very short time scales**.
- When the laser-matter interaction occurs, a burst of UV and soft X-ray radiation is emitted.
  - This is recorded by the detector as the **photopeak**, which defines the absolute time reference t_0
- Subsequentially, the ion signal is detected: first protons, followed by heavier ions.
- Different detectors are employed as ToF: **IC, Scintillator+PMT or Semiconductors**

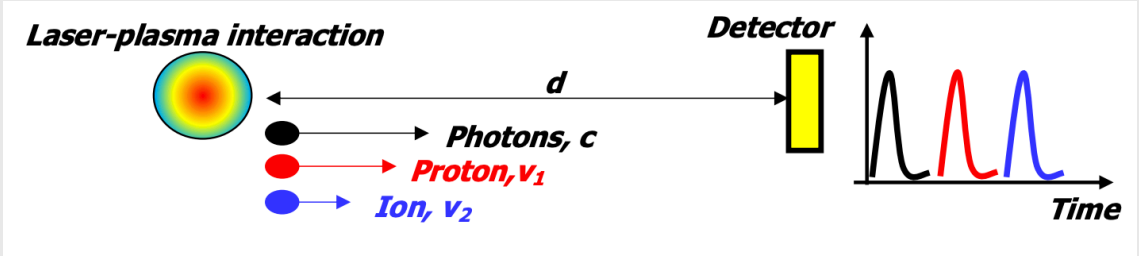

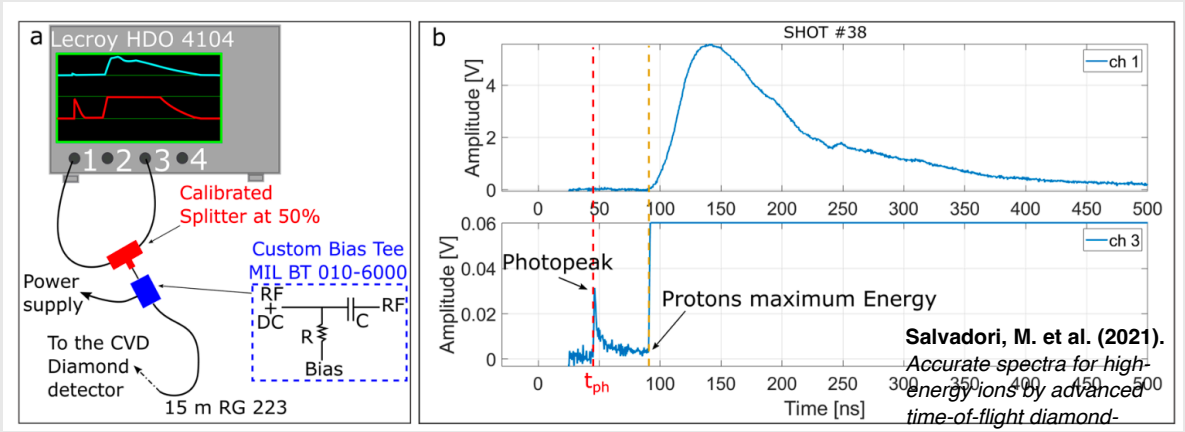

Salvadori, M. et al. (2021). *Accurate spectra for high-energy ions by advanced time-of-flight diamond-detector schemes in high-intensity laser experiments. Sci. Rep.*, **11**, 3071.

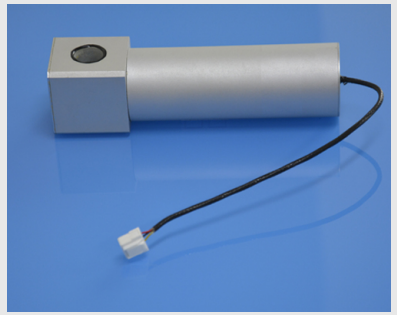

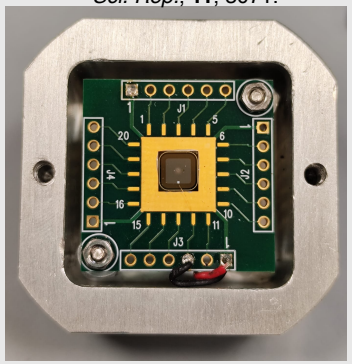

TOF: challenges in laser driven experiment

- **Strong electromagnetic pulse (EMP)** and X-ray background can distort the TOF signal
- **Overlap of ion species** complicates accurate spectrum reconstruction
- **High dynamic range of the signal**

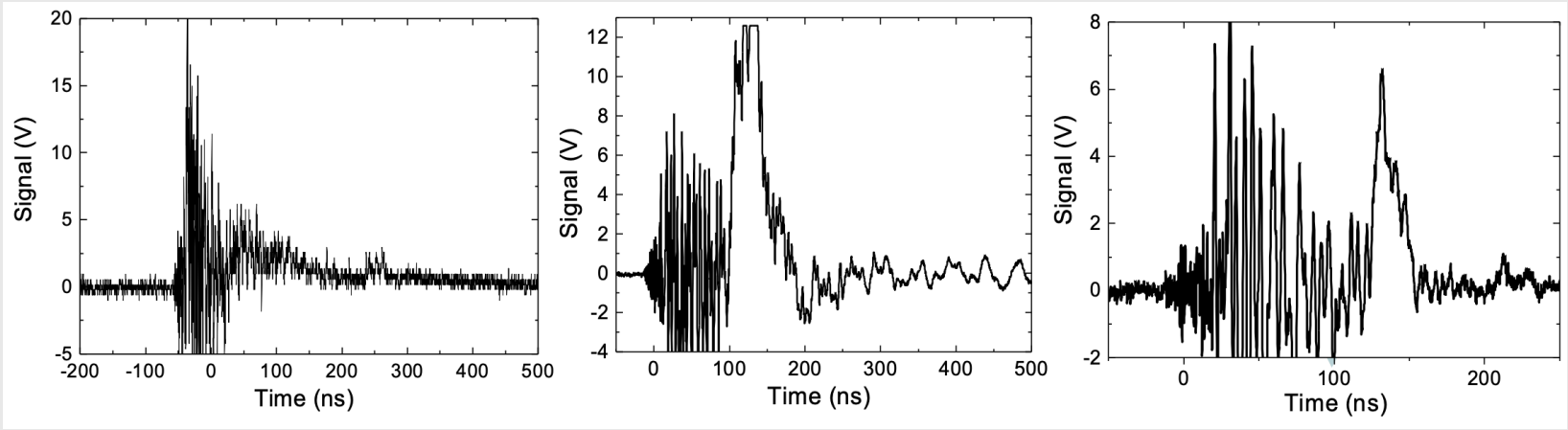

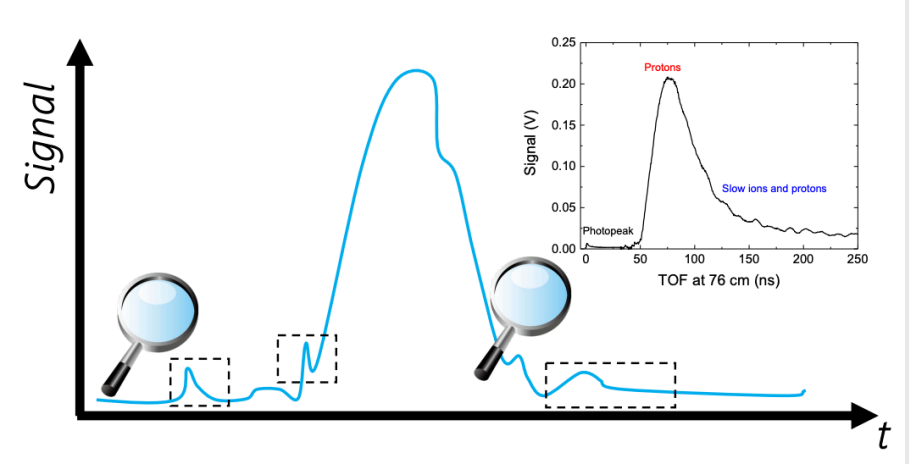

TOF: analytical spectrum computation

- For each temporal step:
  - Energy of the incoming radiation (assuming particle type):

$$E_i = \frac{1}{2} m_p \left(\frac{L}{t_i} \right)^2$$

  - Charge produced: $Q_i = \int_{t_1}^{t_2} \frac{V_i(t)}{R}\, dt$, where the temporal step is defined by the temporal response of the detector
- The number of ions striking the detector is:

$$N_i = \frac{Q_i \epsilon_g}{\eta(E_i)\, E_i\, q_e}$$

Where $\eta(E_i)$ is an efficiency term that counts for the charge collection efficiency of the detector and the fact that because of filters and detector thickness the deposit energy in the detector is not equal to the original energy of the particle

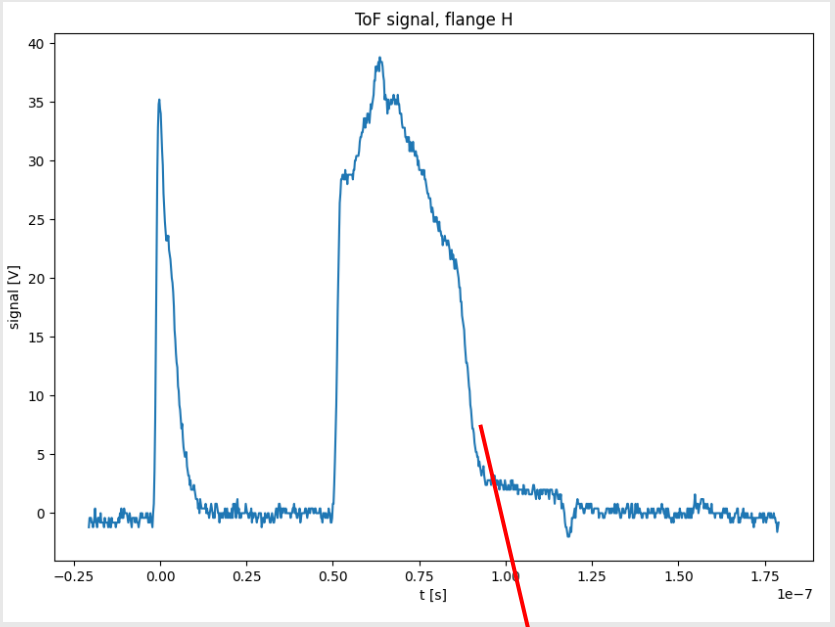

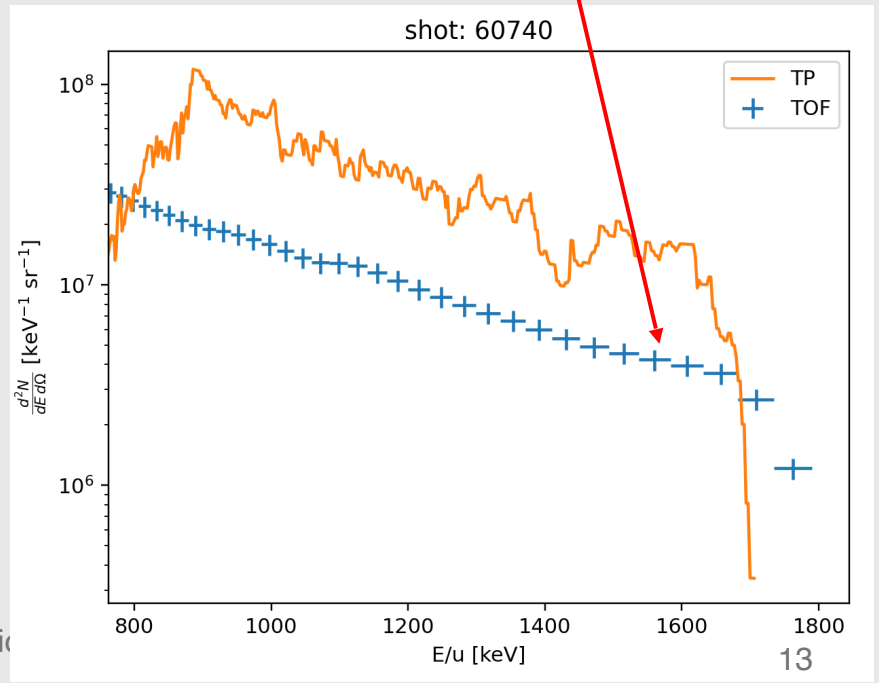

TOF: pure spectrum computation and signal deconvolution

Pure proton spectrum contribution

- In general, it is not possible to distinguish different ion species in the overall ToF signal
- In TNSA acceleration regime, all ions are accelerate by same potential drop
- A time window

$$(t_{p,max} - t_{p,max} + \Delta t_p)$$

with

$$\Delta t_p = t_{p,max}(\sqrt{2} - 1)$$

can be identified, where the signal is dominated by protons.

- In the energy domain. This corresponds to the range:

$$(\frac{E_{p,max}}{2}, \ E_{p,max})$$

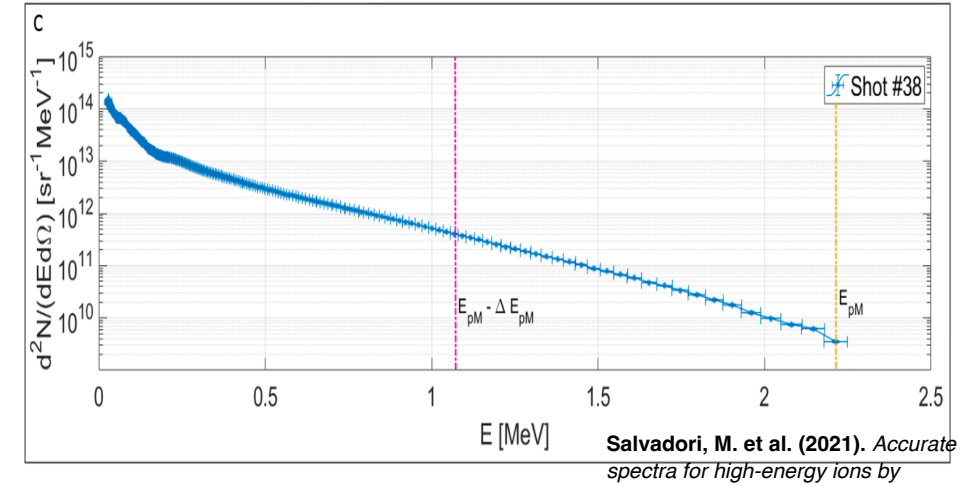

Salvadori, M. et al. (2021). *Accurate spectra for high-energy ions by advanced time-of-flight diamond-detector schemes in high-intensity laser experiments. Sci. Rep.*, **11**, 3071.

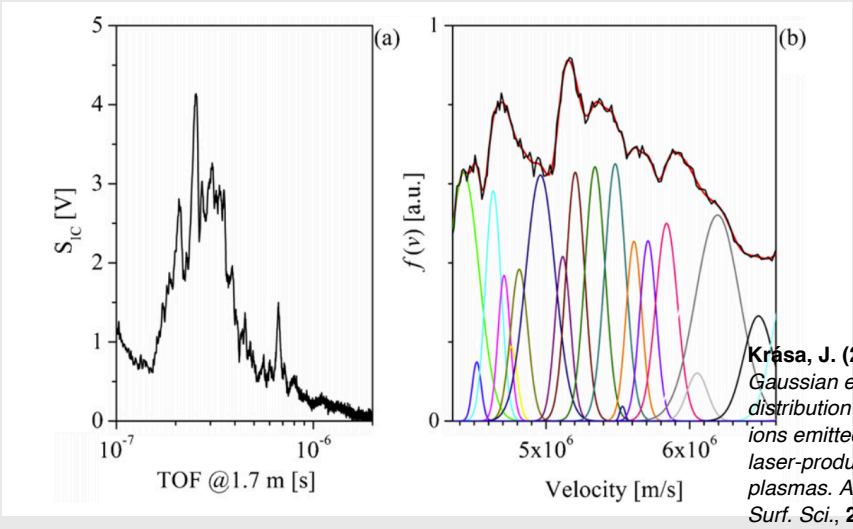

Krása, J. (2013). *Gaussian energy distribution of fast ions emitted by laser-produced plasmas. Appl. Surf. Sci.*, **272**, 46–49.

Signal deconvolution

- Motion of particles is well described by Shifted Maxwell-Blotzman distribution (SMB)
- The detector signal can be described as

$$S(L,t) = \frac{L^{\alpha+1}}{t^{\alpha+4}} \sum S_{i,0} \exp\{ - \frac{m}{2kT_i} \left(\frac{L}{t} - u_i \right)^2 \}$$

2016
Exp campaign at PALS with **thick target**

2017
Exp campaign at PALS with **thin target**

2020
Exp campaign at PALS comparing the **two scheme**

2024
Exp campaign at PALS **double scheme** with new sets of target

2025
Exp campaign at PALS **double scheme**

The INFN Experience on p-11B with sub-nanosecond laser

2022
PROBON O
Cost Action

2023
FUSION project

Nicolò Macaluso - nicolo.macaluso@dfa.unict.it
nicolo.macaluso@lns.infn.it

Activity at PALS Asterix laser facility

Laser characteristics:

- Iodine Gas Laser
- $\lambda = 1.315\ \mu m$
- Pulse duration: [**200 – 350 ps**]
- Delivered energy on target: less then **1 kJ (200-500 J)**
- Intensity on primary target: $[10^{15} - 10^{16}\ W/cm^2\ ]$
- Low repetition rate: about one shot every **25 minutes**

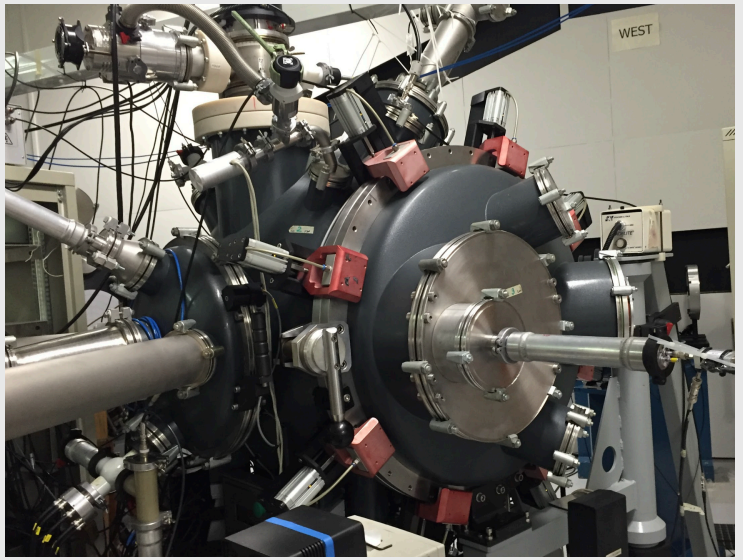

https://www.pals.cas.cz/

Nicolò Macaluso - nicolo.macaluso@dfa.unict.it
nicolo.macaluso@lns.infn.it

2016-2017 experiments using thick NB targets

- Observation of α particle energy spectrum shift toward high energies – possibly due to **post acceleration process in the backward direction**
- High α yield recorded ~ $10^{11} \frac{\alpha}{shot}$

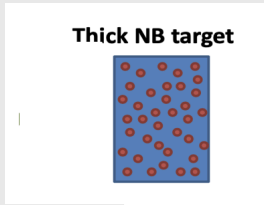

1-0.5 mm

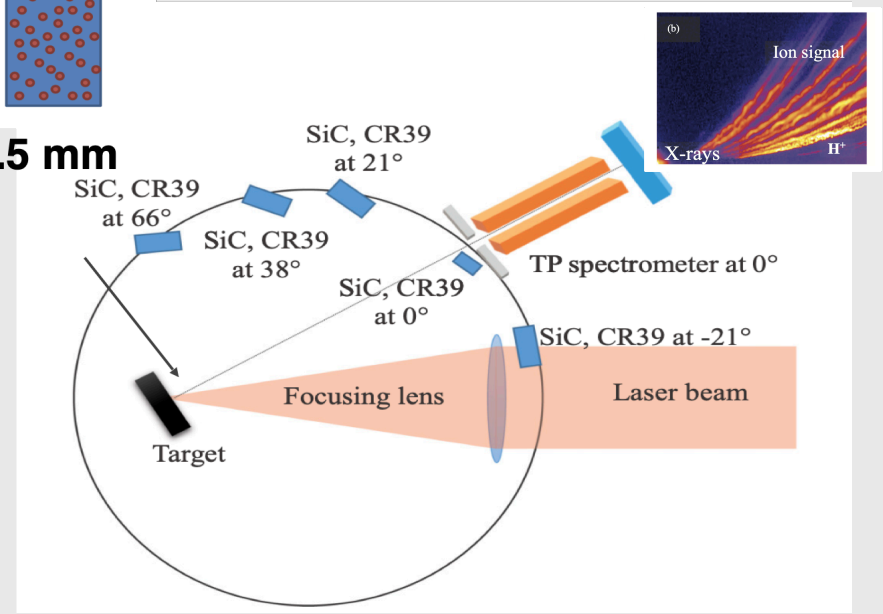

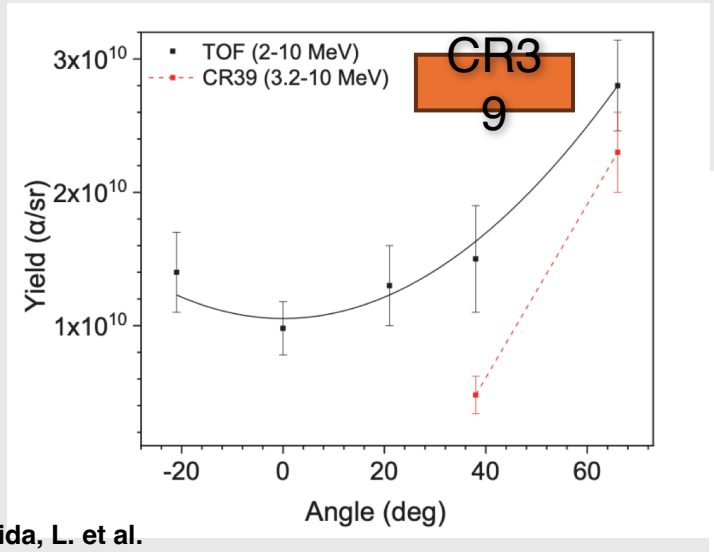

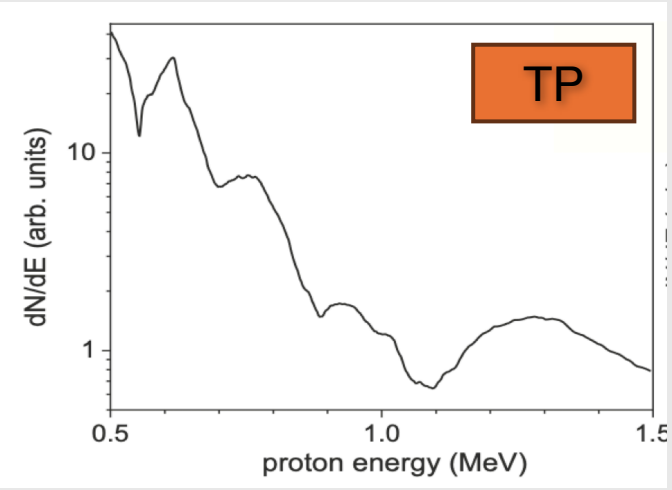

Giuffrida, L. et al. (2020). *High-current stream of energetic α particles from laser-driven proton–boron fusion. Phys. Rev. E*, **101**(1), 013204.

ToF

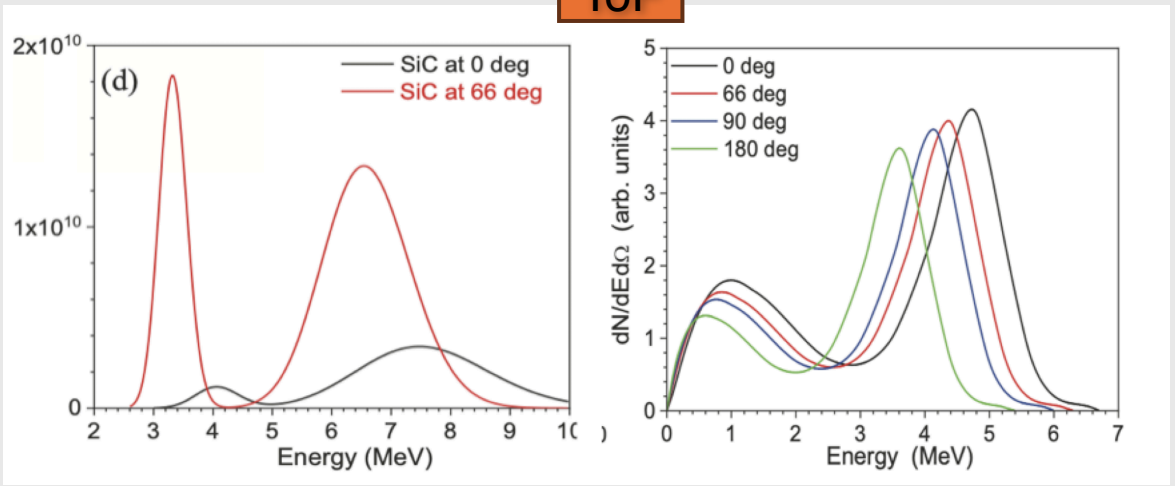

2017 experiments using thin Borated targets

- **Post acceleration** mechanism was **confirmed**
- High α yield recorded ~ $10^9 \frac{\alpha}{shot}$

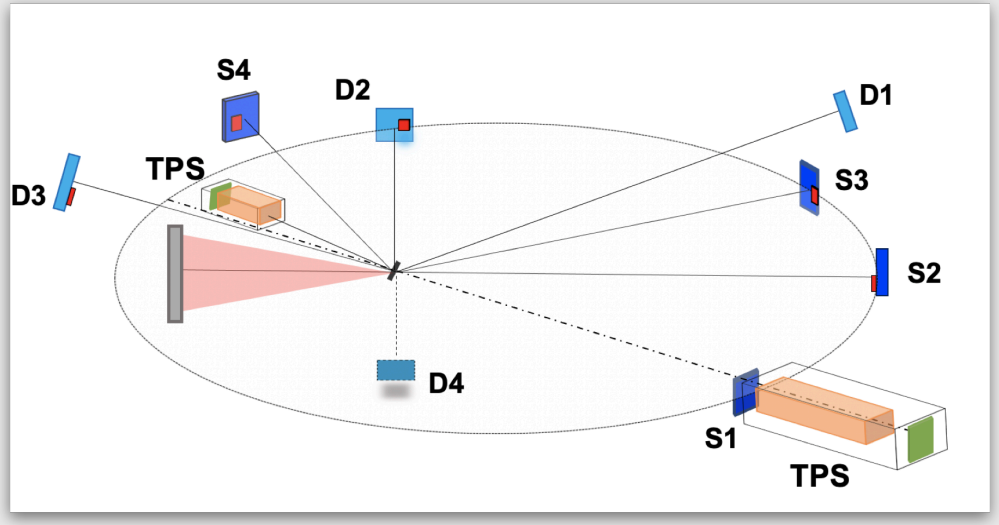

Milluzzo, G. et al. (2023). *Extended characterization of alpha particles via laser-induced p–¹¹B fusion in hydrogenated boron-doped silicon targets. J. Instrum.*, **18**(07), C07022.

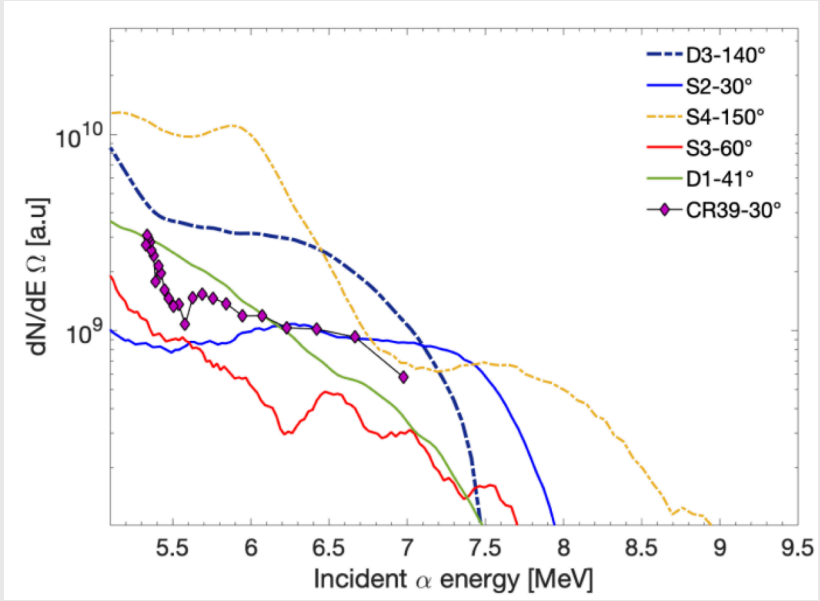

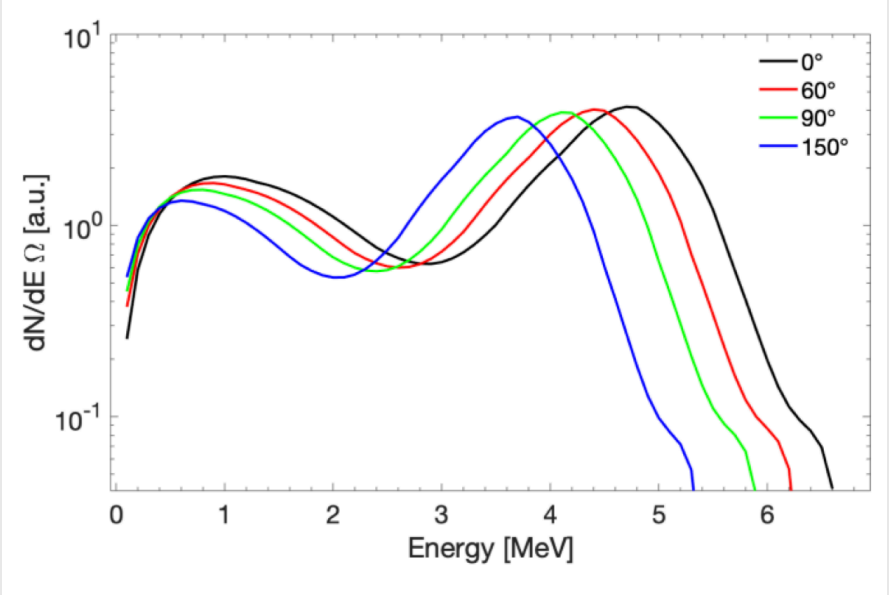

PALS 2024

- Double scheme adopted: **in-target and pitcher-catcher**
- Different type of target employed: **PMMA + Boron, AB and foam**
- Great set of different diagnostic employed: **CR39s, ToF, TP, Electron Spectrometers and HPGe**

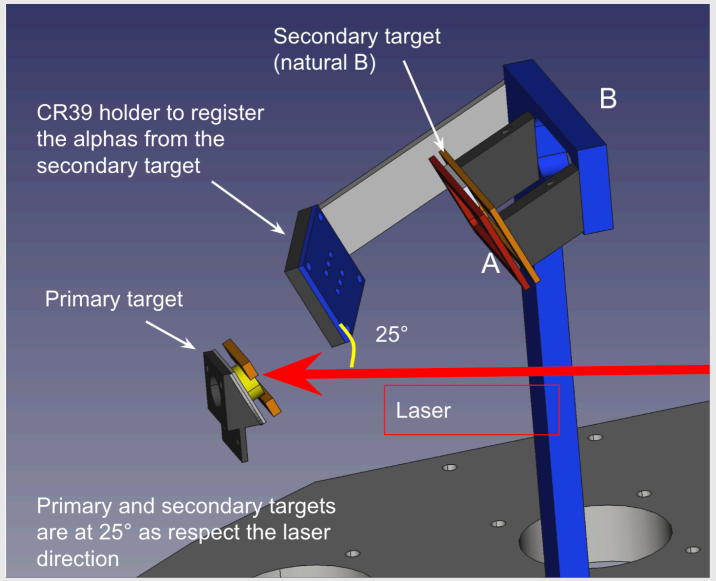

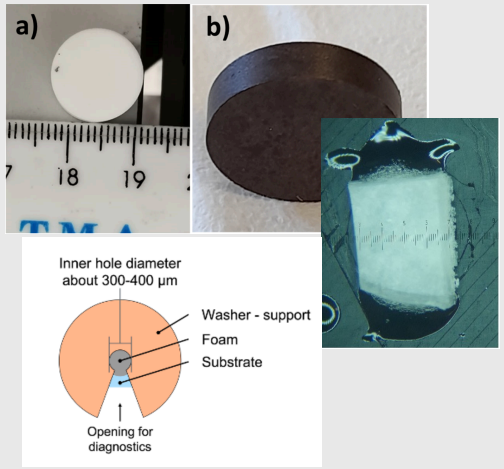

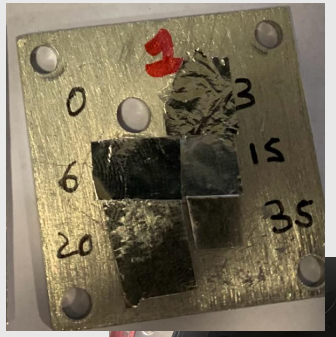

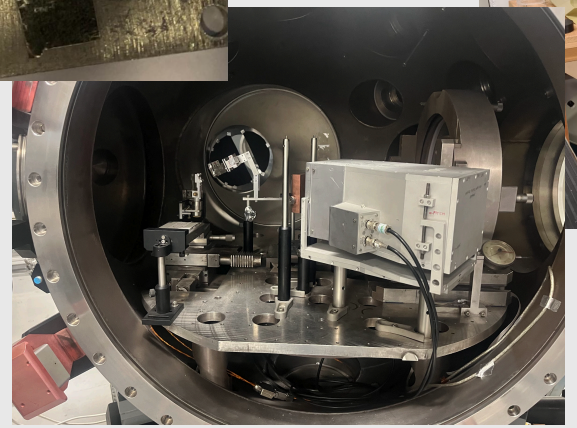

PALS 2024: some results

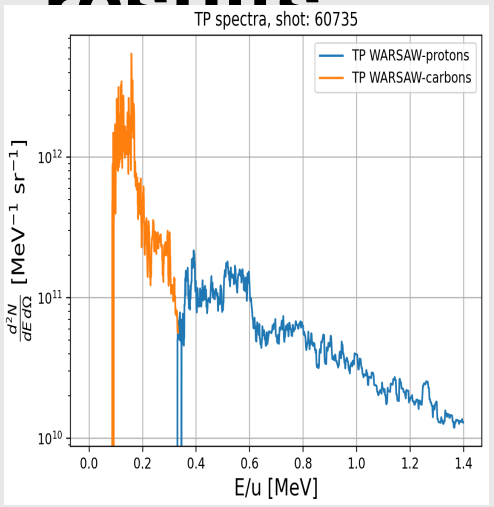

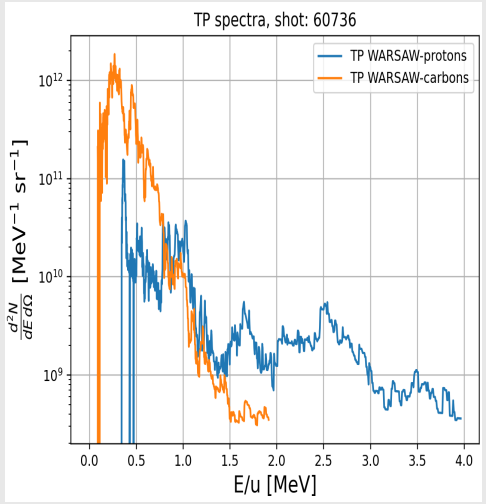

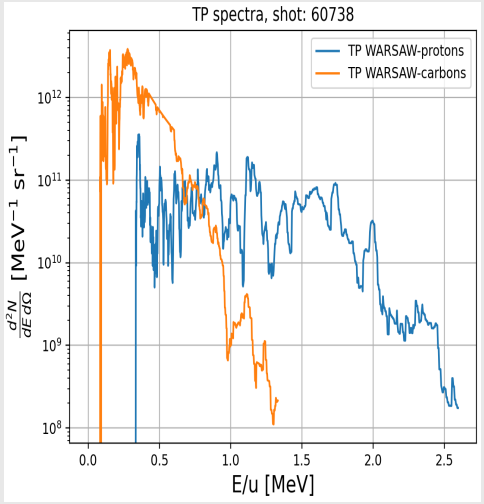

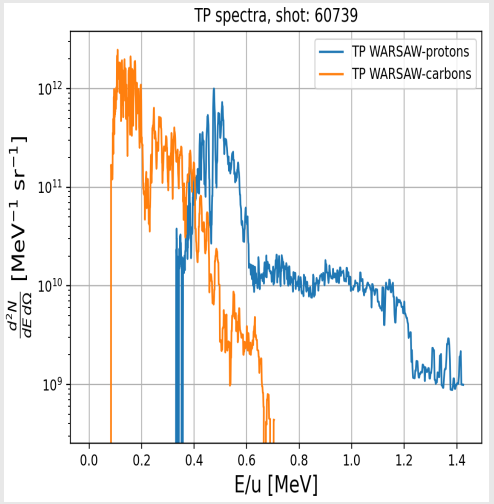

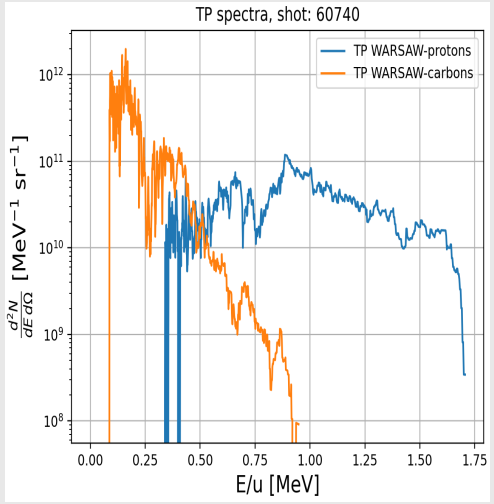

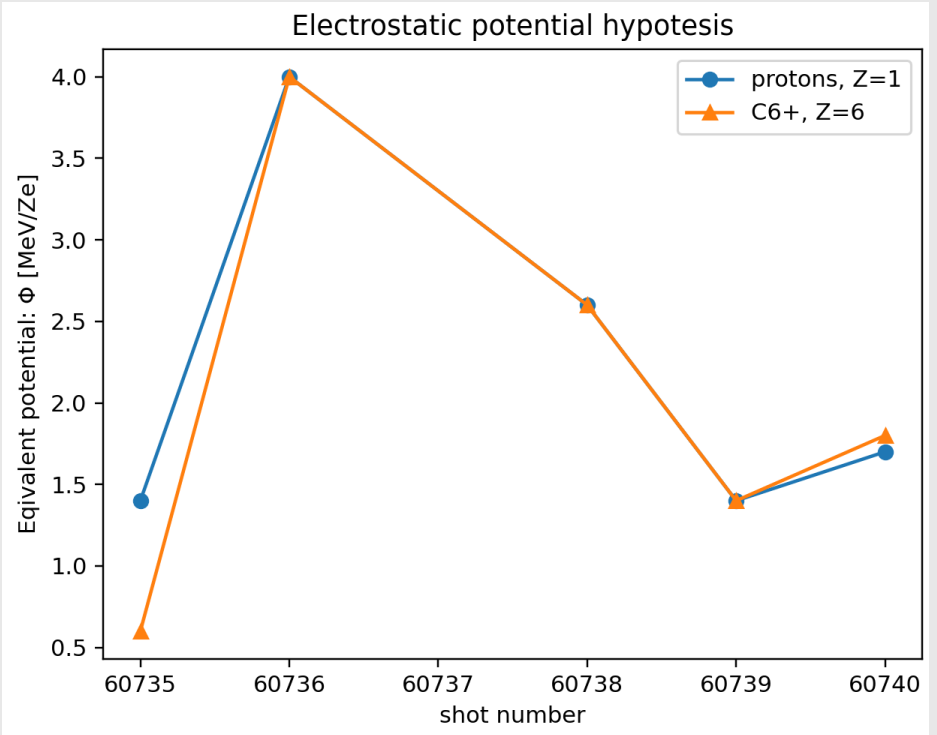

PALS 2024: some results

In-Target:

- ➢ High proton energy in backward direction up to **6 MeV** (with TP and ToF)
- ➢ Self focusing phenomenon

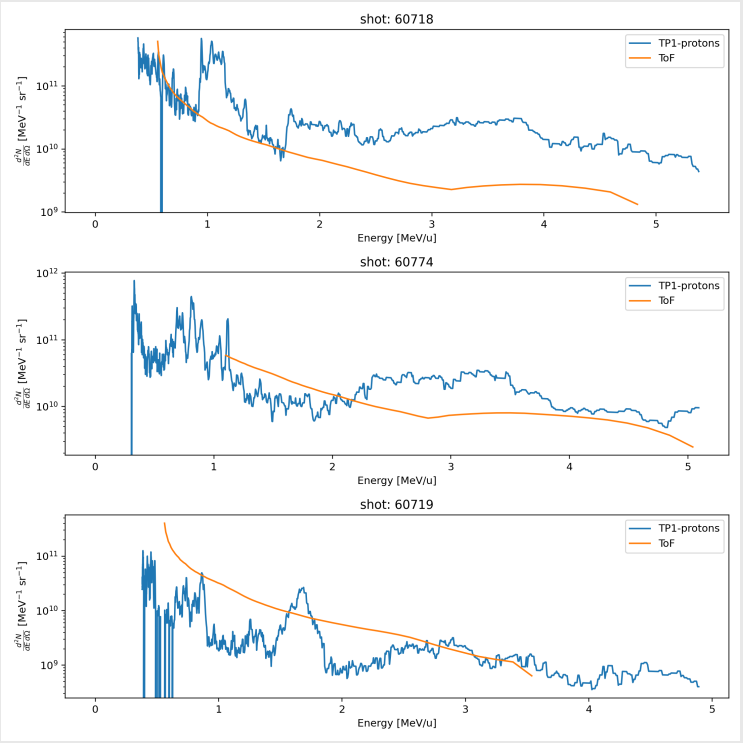

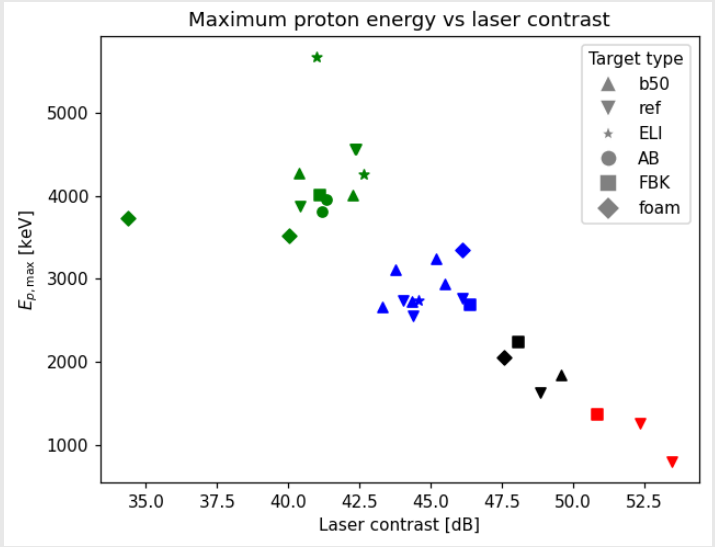

Pitcher-Catcher:

- ➢ Measure the activation of secondary target made of natural boron
- ➢ Estimate α yield ~ $10^7 \frac{\alpha}{shot}$
- ➢ CR39 analysis still ongoing

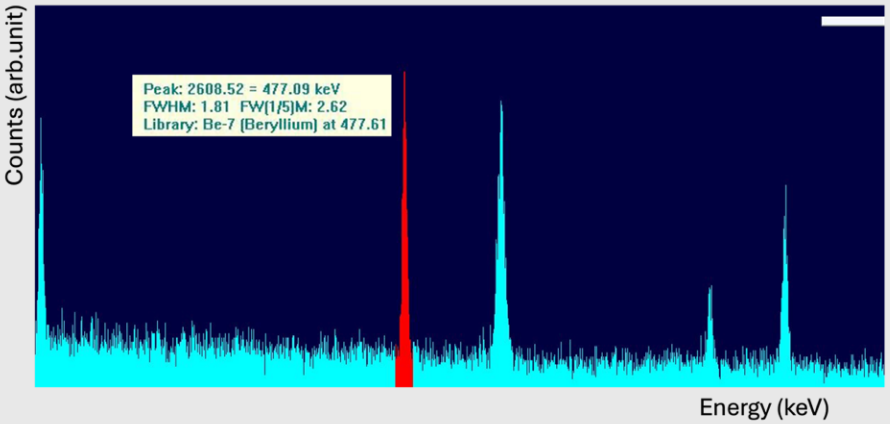

Nicolò Macaluso - nicolo.macaluso@dfa.unict.it
nicolo.macaluso@lns.infn.it

Conclusion:

- Ten years of laser-driven experiment experience paved the way for the INFN laser facility **I-LUCE.**
- **I-LUCE** will be a unique facility where **conventional** and **laser-driven acceleration** coexist.
- It offers great opportunities **for laser-matter interaction studies** and **application** in both **medical physics** and **Inertial Confinement Fusion (ICF)**

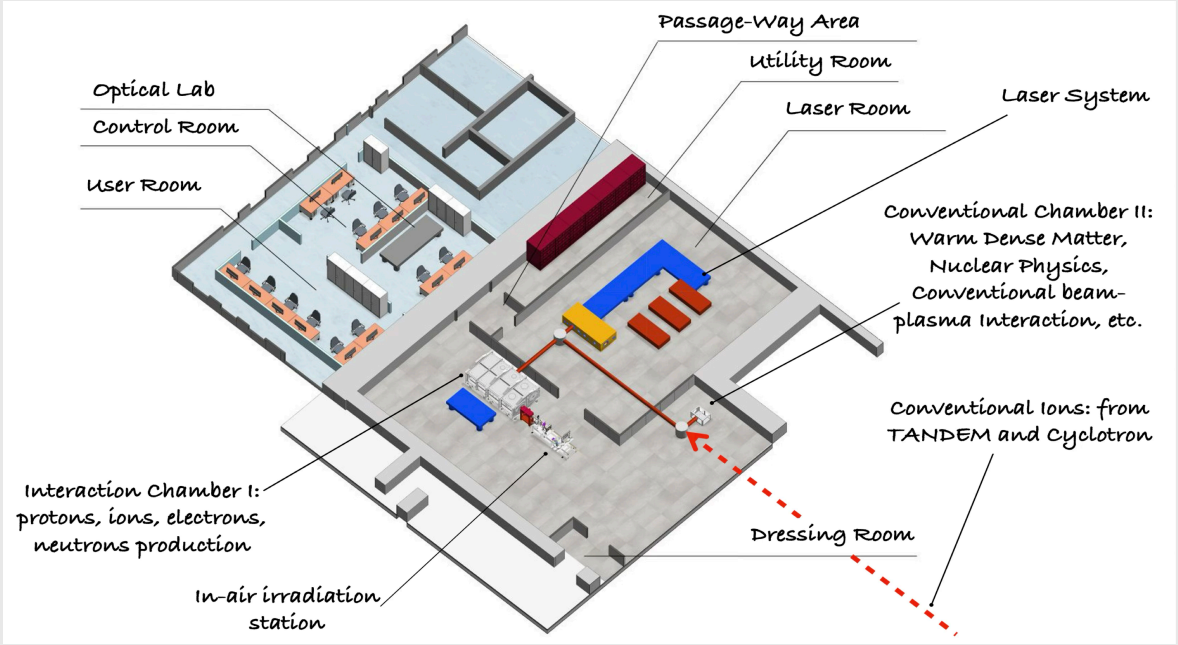

COHERENT L1

Laser Power	< 260 GW
Laser Energy per Pulse	5 – 9 mJ
Laser Pulse Duration	> 35 fs
Laser Intensity	–
Repetition Rate	1 kHz
Plasma Density	–

THALES L2

Laser Power	45 – 320 TW
Laser Energy per Pulse	1.5 – 8 J
Laser Pulse Duration	23 – 25 fs
Laser Intensity	–
Repetition Rate	2.5 – 10 Hz
Plasma Density	–
Strehl Ratio	>80% with Deformable Mirror

Nicolò Macaluso - nicolo.macaluso@dfa.unict.it
nicolo.macaluso@lns.infn.it

Thank you for your attention!

Nicolò Macaluso - nicolo.macaluso@dfa.unict.it
nicolo.macaluso@lns.infn.it